Sports Engineering (2026) 29:10
https://doi.org/10.1007/s12283-026-00539-6

METHODOLOGY

Functional loading validation method of a wireless three-axis force sensor integrated into a cycling pedal

Thomas Chevallier[1,2] · Laetitia Fradet[3] · Jean-Philippe Boucher[2] · Marie Segol[2] · Nicolas Vignais[4]

Received: 19 March 2025 / Revised: 29 December 2025 / Accepted: 1 January 2026 / Published online: 18 March 2026
© The Author(s) 2026

Abstract
This study aimed to propose and apply a validation method for a novel three-axis force sensor integrated into a cycling pedal, which offers several innovative features, notably compatibility with any bike or stationary cycle and fully wireless operation. A measurement rig was designed to compare the outputs of the pedal forces sensor with those of a reference sensor. A functional loading protocol—during which the pedal forces sensor was tested in seven different orientations—was performed to assess the pedal forces sensor validity in both directions of each axis. Data from the pedal forces sensor and the reference sensor were compared using difference plot, mean bias, intra-class correlation, correlation coefficient and root mean squared error. The maximum root mean squared error was observed for the normal axis (20 N). The validation method indicates that the pedal forces sensor demonstrated excellent agreement with the reference sensor for foot pedal reaction forces measurement and could be adapted to other force sensors.

Keywords Force sensor · Cycling · Pedals · Validation · Biomechanics

1 Introduction

In professional cycling, performance can be quantified using a measurement of forces developed by the athletes [1, 2]. Forces generated have thus been linked to pedaling efficiency [3, 4], energy consumption [5, 6], joint angles [7, 8], and muscle activation patterns [4, 9]. Force measurements are also commonly used as inputs for biomechanical models to obtain joint loads, which are then analyzed to understand injury mechanisms, by studying the influence of bike settings or body positions [10–13].

Under real-world track cycling conditions, according to Drouet et al. [14], peak normal forces perpendicular to the anteroposterior axis can reach up to 2200 Newtons (N) during the downstroke and around −400 N during the upstroke. In the anteroposterior (AP) direction, forces typically range from −500 to +600 N. According to Martin-Sosa al. [15], medio lateral (ML) forces range from −50 to 100 N during low intensity pedaling tasks.

Force sensors are therefore critical in this kind of investigation. Those used in cycling are mainly made of strain gauges [16] arranged in specific patterns and connected to form a Wheatstone bridge circuit. When force is applied, the material undergoes a deformation that changes the electrical resistance of these strain gauges. This change in resistance is therefore proportional to the magnitude of the force applied, enabling quantification of the force exerted on the pedal.

Most instrumented pedals are not capable of measuring the three-axis foot-pedal interaction in real time without compromising the rider's movement or altering the bicycle setup. Traditional force sensors are typically limited to laboratory use due to wired data acquisition systems [14, 15, 17, 18]. Some commercially available systems such as the Assioma (Favero Electronics, Italy), Keo Blade Power (Look, France) and Rally (Garmin, US) offer wireless measurement but are restricted to propulsive power measurement and limited in data acquisition frequency. Dieltiens et al. [17] proposed a three-axis pedal sensor that could be mounted on any standard bicycle, but the setup still required the cyclist to wear a backpack containing the data

✉ Thomas Chevallier
thomas.chevallier@phyling.fr

1 CIAMS, Université Paris-Saclay, 91405 Orsay, France

2 Phyling, 91120 Orsay, France

3 Lab-STICC, UMR 6285, CNRS – Université de Bretagne Sud, 56100 Lorient, France

4 Univ Rennes 2, Inria, M2S, 35000 Rennes, France

acquisition system. Other systems, such as the crank-based design presented in refs [15, 18], integrated three-axis force sensors into the crankarm rather than the pedal itself. While promising, these approaches remain constrained to laboratory use and are less 'plug and play'.

Validation studies are carried out to assess the confidence of these new sensors data. For this, quantification of these force sensors measurement errors during cycling are often performed in static rather than dynamic conditions [15, 19, 20]. Static conditions are characterized by constant loads, such as calibrated masses, while dynamic conditions involve loads that vary over time. In dynamic conditions, validation strategies from the literature relied on indirect metrics such as power values or pedaling indicators such as the angle at which the maximum force is developed [19]. In contrast, Falda-Buscaiot et al. [21] proposed a direct and dynamic validation procedure for each axis of a force sensor used during skiing, comparing the sensor outputs directly with those obtained from a reference sensor under variable conditions. In this protocol, the tested force sensor was integrated into a ski boot and fixed to a force platform to compare the outputs.

Other critical points in validation studies are the metrological characteristics that are assessed to validate the sensors. It is well known that metrology and force sensor validation should include specific characteristics such as accuracy and repeatability [16], which are pivotal to validity and consistency of data collection. Accuracy refers to how closely the sensor measurements align with the true values of the forces being measured. In cycling studies, accurate sensors are needed to precisely capture the forces exerted during pedal strokes. Repeatability denotes the ability of the sensor to produce consistent measurements when the same force is applied many times, highlighting the capacity of the sensor in replicating results. Bouillot et al. [16] listed protocols, metrological variables of interest, and statistical tests used in 74 studies. According to this study, the statistical parameters commonly used to compare two measurements are t-test, correlation coefficients (CC), limits of agreements (LOA) and Root Mean Squared Error (RMSE).

In this context, after detailing a method for calibrating a force sensor, the present study addresses two main objectives: first, to describe a method for validating a novel wireless three-axis force sensor integrated into cycling pedals, and second, to apply this validation methodology. This approach aims to provide a solution for assessing the accuracy of force sensors used in biomechanical analysis.

2 Materials and methods

The investigation focused on a commercially available three-axis pedal force sensor (PI3D; Phyling, France), instrumented with twelve strain gauges (Kyowa KFGS-2–120-C1-11, Japan) arranged in full Wheatstone bridges (4 strain gauges per axis) wired to an electronic unit (Mini-Phyling V1, Phyling, Palaiseau, France) placed on the front of the PI3D, which integrated all acquisition electronics, signal conditioning, and wireless transmission modules. The angle of the PI3D was computed using a combination of a magnetometer and a gyroscope integrated into the Mini-Phyling V1. The PI3D measures forces along the three axes illustrated in Fig. 1.

For each axis, the positive directions were defined as + AP, + ML, + N and the negative ones as -AP, -ML and -N. The data acquisition frequency was set at 200 Hz. The PI3D was equipped with: (i) a fixation cleat to measure forces exerted during the PI3D calibration, and (ii) a cycling cleat presented in a previous study [14] to measure forces exerted during a pedaling task.

2.1 Calibration procedure

This section describes the calibration procedure used to define the model required to convert raw data from PI3D to force values.

To characterize the full three-axis sensitivity of the PI3D, it was locked in three different orientations on a measurement rig (Fig. 2A), each aligning one of the three measurement axes (AP, ML, N) with the vertical direction of the applied load. For each of these three orthogonal orientations, five calibrated masses (10 kg, 20 kg, 30 kg, 40 kg, 50 kg) were applied for 30 s. During each application, the voltage outputs from all three measurement axes (AP, ML, N) were simultaneously recorded. This data collection enabled characterization of the direct response to force along an applied axis and any transverse sensitivity. By analyzing these cross-axis responses across all orientations and loads, the sensitivity matrix was computed. This matrix (M) was obtained using least squares optimization to minimize the residuals between the measured input voltage signals (I) and the expected output forces (O), as represented by the equation $M \times I = O$. This procedure enabled conversion of raw PI3D signals into corrected three-axis force components. The maximum normalized root-mean-squared error (nRMSE) remained below 0.1%. This methodology compensated for potential manufacturing imperfections or misalignments, ensuring improved accuracy when measuring forces along each axis.

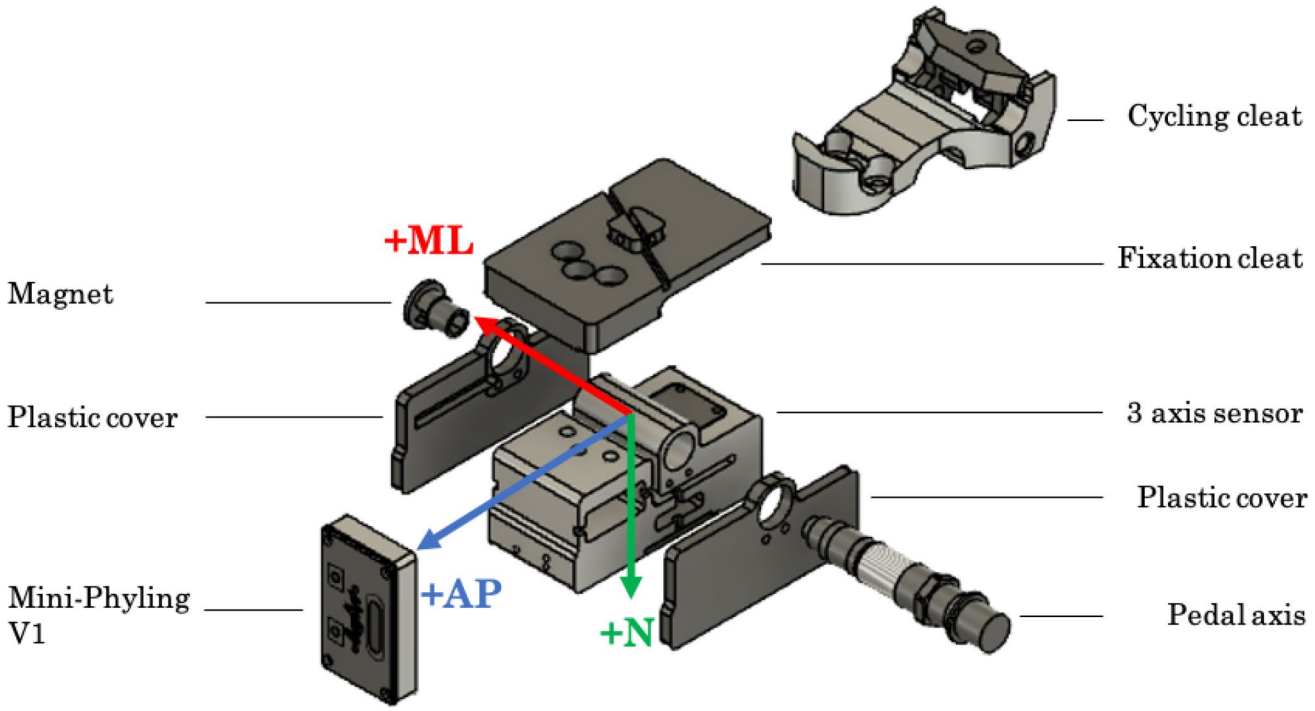


Fig. 1 Exploded view of the PI3D. The PI3D measures forces along three axes, defined as the antero-posterior (AP), medio-lateral (ML), and normal (N) axes. The Mini-Phyling V1 is an electronic unit that contains a gyroscope, a magnetometer and collects data from the PI3D. The cycling cleat corresponds to the design of the Look brand (Nevers, France), which commercializes pedals and cleats for cycling. The fixation cleat was inspired by a design presented in a previous study [14] and enables the attachment of rigid wires for calibration and functional loading measurements

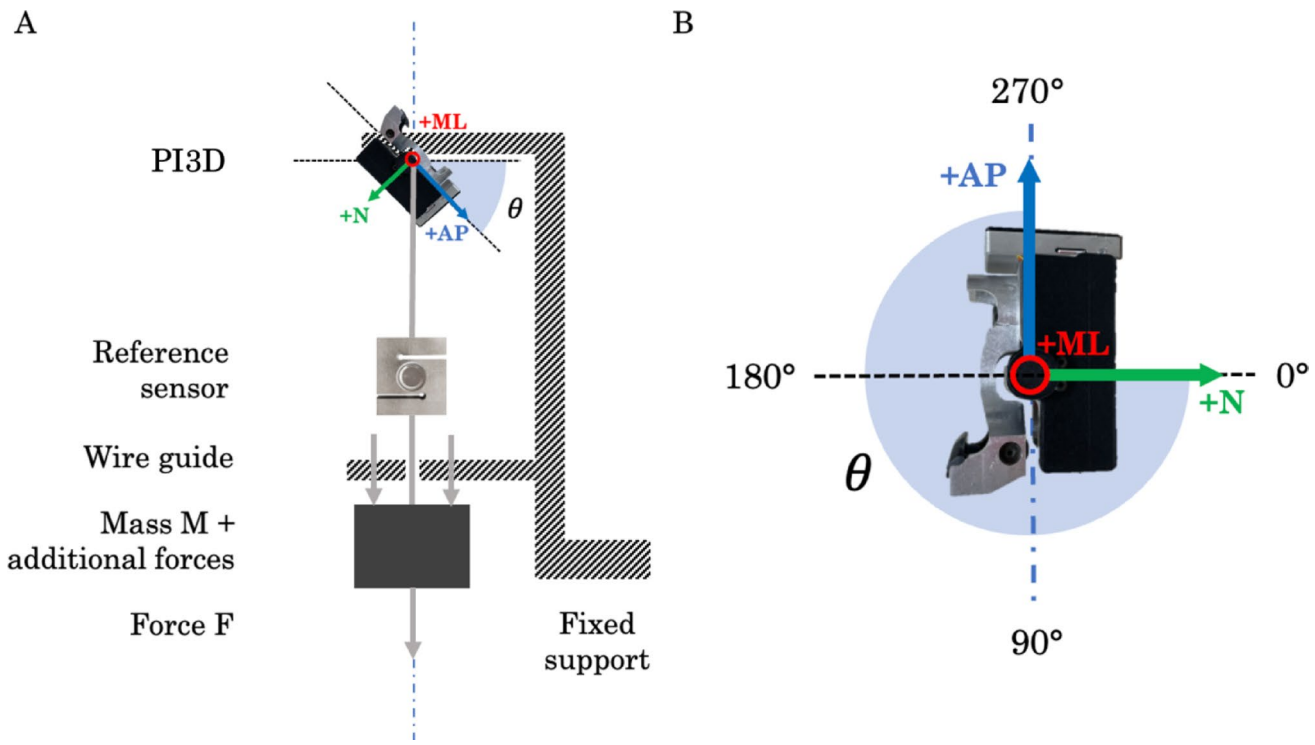


Fig. 2 **A** Schematic representation of the measurement rig. In this configuration, the total force measured was a combination of the N and AP axes for the PI3D and corresponded to the force measured by the uniaxial RS. **B** Zoom on the PI3D orientation: in this configuration, a clockwise rotation of 270° was applied around the ML axis. The rotation was applied from the initial position where the+AP axis was pointing to the 0° position

2.2 Force sensor validation protocol based on a functional loading procedure

The experimental setup and functional loading procedure used to assess the validity of the PI3D are described in this section. Measurements obtained with the PI3D were compared to those obtained with a reference sensor (RS), specifically a single-axis force sensor SM5424 (Sensel Measurement, Vincennes, France). The RS provided a measurement range up to 10 kN with a manufacturer-stated accuracy of 0.1%, which complies with ISO 376 standards. The data-acquisition frequency was 1000 Hz for the RS.

A custom-designed measurement rig was developed to evaluate the PI3D performance (Fig. 2A). The rig included a fixture designed to hold the PI3D by its pedal axle. This fixture was fastened to the rig to rigidly fix the PI3D in a chosen orientation, as described in Table 1. The theta angle (θ) represented the rotation around the ML axis from the 0° orientation, defined as the configuration in which the AP axis of the PI3D was aligned with the horizontal axis of the reference frame (Fig. 2B). The fixation cleat enabled attachment of a 2-mm-diameter steel wire linking the PI3D to the RS.

After placing the PI3D on the rig, its orientation was measured with an inclinometer to achieve the targeted θ angle (Fig. 2B). Force orientation was guided by a wire guide. To simulate pedaling conditions, a baseline load of 200 N was used. This value was chosen based on preliminary experimental trials to ensure stable and reproducible loading. Additional manual forces were applied to reproduce the variability and amplitudes observed during functional pedaling. This setup provided a controlled environment, allowing the operator to apply additional forces along the wire to reproduce loading patterns closer to cycling conditions. The ML axis was not tested because the rig could not be safely adapted to apply forces in this direction.

A cycle of force application was defined as a rise to the target force (Table 1) followed by a return to the 200 N baseline. Target forces were based on track cycling force values [14] although the manual procedure did not guarantee that these values could be fully reached.

To generate forces greater than 600 N, the operator loaded a 200 N mass and manually dropped it from ten centimeters to generate peak forces up to 2000 N. This drop-mass procedure produced high loading rates (Appendix 1, Fig. 1), but it did not reflect the temporal characteristics of real pedaling dynamics. The loading rate during this procedure was about ten times higher than that typically experienced during cycling. This process was used for the condition assessing the positive normal axis (+N), corresponding to the configuration in which maximum force is applied to the pedal [14].

Two combined loading conditions (AP/N) were performed to mimic cycling pedal forces. The combination of AP and N forces represented propulsive forces [15]. A measurement condition consisted of twenty cycles, a number chosen for statistical stability and experimental practicality based on preliminary analyses. The two functional load patterns are presented in Appendix 1.

2.3 Data treatment for the force sensor validation

Data from the PI3D were resampled to 1000 Hz to match the RS acquisition frequency. A 5th-order Butterworth low-pass filter with a cut-off frequency of 50 Hz was applied to both PI3D and RS signals to remove high-frequency noise while preserving the signal. A higher cut-off frequency than typically used in pedal force studies (6–20 Hz) [3, 22] was selected to ensure that the high-frequency components generated by the manual drop-mass procedure were not attenuated. To achieve temporal synchronization between the two measurement systems, a cross-correlation function was used. This method enabled accurate and stable synchronization between the two signals, supporting comparison under varying loading conditions.

To quantify the agreement between PI3D and RS measurements, a Bland–Altman analysis was performed on all collected values from each of the 20 functional loading cycles to compute the bias between PI3D and RS. Due to the characteristics of time-series data and observed heteroscedasticity (non-constant variance) in the differences, traditional fixed Limits of Agreement (LoA) were not applied [23]. Instead, the raw scatter of differences was presented to illustrate the variation in agreement across the measurement range (Fig. 3).

Intra class correlation ($ICC_{(3,1)}$, two-way mixed effects, consistency, single measurement) analysis [24] was conducted on the peak force of each cycle to determine the agreement between PI3D and RS for extreme values. In addition, the correlation coefficient (CC) and the root-mean-squared

Table 1 Experimental conditions for force application cycles, where the axis was the component and the direction loaded, Angle θ corresponded to the rotation around the ML axis on the measurement rig. Force max was the targeted force to reach at each cycle

	Conditions						
Axis	+AP	+AP/+N	−AP	−AP/−N	+ML	+N	−N
Angle θ	90°	45°	270°	225°	0°	0°	180°
Target force max (N)	600	600	600	600	600	2000	600
Number of repetitions	20	20	20	20	60	20	20

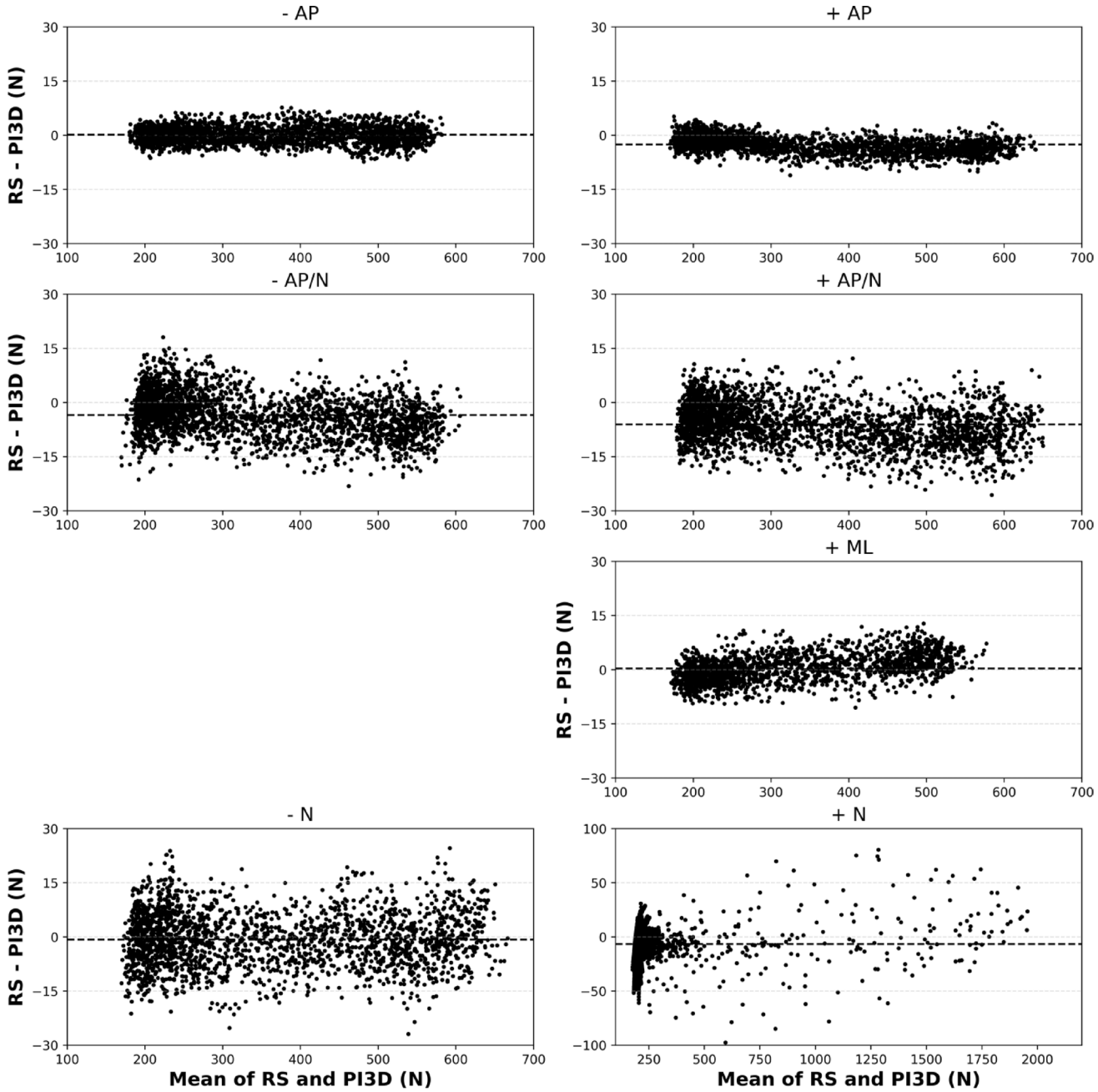


Fig. 3 Difference plot for each loading condition. Each point represents the difference between the force values measured by the RS and the PI3D, plotted against the corresponding RS value. The dotted line represents the mean bias between the two measurements

error (RMSE) were calculated over each cycle between the force measured by the two sensors to assess force-measurement accuracy and to facilitate comparison with previous studies.

3 Results

Table 2 presents the mean peak values and standard deviations (SD) for the RS and the PI3D, along with the intraclass correlation results (ICC(3,1)) and the bias between PI3D and RS. The values corresponded to the mean peak forces measured during the different functional loading conditions are described in Table 1.

The mean bias (Table 2) and difference plot (Fig. 3) showed a high level of agreement between the peak values

Table 2 Peak values and SD for RS and PI3D, ICC (ICC values for each pair of peak values between PI3D and RS), mean bias RS/PI3D and range of values (min, max), CC and RMSE for each condition

Axis	RS peak ± SD (N)	PI3D peak ± SD (N)	$ICC_{(3,1)}$	Mean bias (min, max) (N)	CC	RMSE (N)
+AP	559 ± 89	556 ± 89	0.99	−2.6 (−11, −5)	0.99	3
−AP	529 ± 65	530 ± 65	0.99	0.2 (−7, 8)	0.99	2
+ML	511 ± 63	514 ± 64	0.99	0.4 (−11, 12)	0.99	4
+N	1660 ± 279	1663 ± 288	0.99	−6.5 (−97, 80)	0.99	20
−N	595 ± 83	602 ± 83	0.99	−0.7 (−27, 26)	0.99	8
+AP/+N	583 ± 93	578 ± 91	0.99	−6.1 (−25, 12)	0.99	8
−AP/−N	544 ± 70	542 ± 69	0.99	−3.5 (−23, 18)	0.99	7

measured by the RS and the PI3D. The error range remained low for AP and ML conditions but increased for the N conditions. The maximum error value reached 20 N in the +N condition.

Furthermore, the differences plot (Fig. 3) indicated that errors at both low and high force values were generally consistent.

4 Discussion

Results indicated a maximal bias below 7 N between both systems, and correlation coefficient (CC) values consistently above 0.99 confirmed a strong temporal similarity across loading cycles. However, such high correlations should be interpreted with caution, as they primarily reflect timing similarity rather than agreement in absolute force magnitudes. Additionally, ICC analysis revealed excellent agreement (ICC > 0.99) [24] in peak force values across cycles, and RMSE values remained low, indicating high measurement accuracy of the PI3D relative to the RS. Altogether, these quantitative findings highlight the robust performance of the PI3D in quantifying multi-directional forces, supporting its future use for understanding biomechanical dynamics in cycling.

For the +N condition, a greater dispersion of errors was observed at higher force magnitudes, suggesting increased variability in that direction. This wider dispersion is partly attributed to the broader measurement range of the +N axis. Time synchronization between the two systems also proved less accurate in this condition, likely due to the short loading duration (≈0.05 s) (Annexe 1). Even a one-frame misalignment despite resampling at 1000 Hz could thus introduce noticeable discrepancies. Additionally, manual loading inherently produced deviations from the targeted force, sometimes resulting in values below 2000 N, which may have contributed to a bias underestimation (Table 2). A linear increase in error across the force range was also observed in the +ML condition, indicating a proportional bias and suggesting that agreement between the PI3D and RS diminishes at higher ML force levels (Fig. 3).

Previous studies validating force sensors integrated into pedals generally reported only results from static protocols, with RMSE values ranging from 2 to 14 N [19, 20, 25–27]. More recent work reported nRMSE values between 1.1% and 3.4% depending on the axis [15]. Sensors developed for other sports showed RMSE values from 14 to 35 N [21], corresponding to a mean nRMSE of 3.2%.

The results of the present study are consistent with these findings, with a maximum RMSE of 20 N (1.5% of the maximal peak force measured). The higher absolute RMSE observed in here is likely linked to the higher force magnitudes used in our procedure (> 500 N).

Test–retest studies quantify the minimal detectable difference (MDD), representing the smallest change that can be considered real [28]. The greatest mean bias identified in the present study (6.8 N) was below the MDD for peak effective force (9 N), and far below that for peak ineffective force (72 N) [29]. However, the maximum PI3D RMSE (20 N) exceeds the MDD for peak effective force, suggesting that the system may not reliably detect subtle changes in this specific parameter. Its use in longitudinal monitoring should therefore be interpreted with caution, particularly when very small changes are of interest.

This study presents several limitations. Regarding materials, safety constraints associated with the drop-mass protocol were necessary to generate high forces, and although a wire guide was used to align loads with the vertical axis, manual application may have introduced directional variability. The protocol evaluated the PI3D in multiple orientations by applying loads across different axes, but the pedal rotation axis was fixed to simplify the experimental setup, which differs from real pedaling conditions. Testing the PI3D with a freely rotating pedal would have been informative. Nevertheless, evaluating multiple configurations (two orientations for the AP and N axes and one for the ML axis) helped minimize bias related to sensor orientation [15].

Additionally, the protocol did not replicate pedaling dynamics. Force cycles were applied under controlled, non-cycling conditions, limiting ecological validity. While this approach enabled repeatable, controlled measurements, it does not capture the complex multi-directional forces observed during real cycling, such as sprinting, climbing,

or rapid cadence changes. Manual loading also introduced variability in targeted amplitudes, and the study did not include comprehensive assessments of measurement repeatability or reproducibility. Future research should include repeated trials under realistic cycling conditions to evaluate PI3D performance and reliability in dynamic environments.

5 Conclusion

This study proposed and implemented a method to validate multi-axis force sensors, with a specific focus on the PI3D developed by some of the authors. Under controlled laboratory conditions, the PI3D demonstrated valid performance for estimating pedal forces. The proposed validation approach provides a practical framework for assessing the accuracy of such sensors in biomechanical research. Thanks to its wireless design, the PI3D may be suitable for use in real-world cycling conditions, although further investigations are required to evaluate field performance. The ability to measure ML forces (non-propulsive forces) during training could for instance provide valuable insights into pedaling biomechanics and help identify movement patterns associated with injury risk.

Supplementary Information The online version contains supplementary material available at https://doi.org/10.1007/s12283-026-00539-6.

Acknowledgements The authors would like to thank the Phyling Team for their help during the development of the PI3D. Specifically, Eric Busquet for the manufacturing of the sensor.

Author contributions LF, NV and TC designed the protocol. TC collected data. TC and JP.B analysed data and prepared tables and figures. MS designed the sensor and the measurement rig. TC wrote the main manuscript, LF and NV reviewed it.

Funding Open access funding provided by Université Paris-Saclay.

Data availability No datasets were generated or analysed during the current study.

Declarations

Conflict of interest The PI3D evaluated in this study was developed by some of the authors as part of a PhD collaborative program between a private company (Phyling) and a public laboratory (CIAMS). This relationship may be perceived as a potential conflict of interest. This is specified in the manuscript.

Open Access This article is licensed under a Creative Commons Attribution 4.0 International License, which permits use, sharing, adaptation, distribution and reproduction in any medium or format, as long as you give appropriate credit to the original author(s) and the source, provide a link to the Creative Commons licence, and indicate if changes were made. The images or other third party material in this article are included in the article's Creative Commons licence, unless indicated otherwise in a credit line to the material. If material is not included in the article's Creative Commons licence and your intended use is not permitted by statutory regulation or exceeds the permitted use, you will need to obtain permission directly from the copyright holder. To view a copy of this licence, visit http://creativecommons.org/licenses/by/4.0/.

References

1. Turpin NA, Watier B (2020) Cycling biomechanics and its relationship to performance. Appl Sci (Switzerland) 10:1–15
2. Dorel S (2018) Maximal force-velocity and power-velocity characteristics in cycling: assessment and relevance. In: Biomechanics of training and testing: innovative concepts and simple field methods. Springer, pp 7–31 ISBN 9783319056333
3. Korff T, Romer LM, Mayhew I, Martin JC (2007) Effect of pedaling technique on mechanical effectiveness and efficiency in cyclists. Med Sci Sports Exerc 39:991–995. https://doi.org/10.1249/mss.0b013e318043a235
4. Dorel S (2018) Mechanical effectiveness and coordination: new insights into sprint cycling performance. In: Biomechanics of training and testing: innovative concepts and simple field methods, pp 33–62, https://doi.org/10.1007/978-3-319-05633-3_3
5. Borszcz FK, Tramontin AF, Bossi AH, Carminatti LJ, Costa VP (2018) Correction: Functional threshold power in cyclists: validity of the concept and physiological responses. Int J Sports Med 39:e1. https://doi.org/10.1055/a-0639-1221
6. Hawley JA, Noakes TD (1992) Peak power output predicts maximal oxygen uptake and performance time in trained cyclists, vol 65. Springer
7. Bini RR, Senger D, Lanferdini F, Lopes AL (2012) Joint kinematics assessment during cycling incremental test to exhaustion. Isokinet Exerc Sci 20:99–105. https://doi.org/10.3233/IES-2012-0447
8. Bini RR, Diefenthaeler F (2010) Kinetics and kinematics analysis of incremental cycling to exhaustion. Sports Biomech 9:223–235. https://doi.org/10.1080/14763141.2010.540672
9. Sachet I (2022) Rôle Des Qualités et Des Coordinations Musculaires Dans'optimisation de La Puissance Maximale En Pédalage, Université de Nantes
10. Ménard M (2016) Effet de La Posture Sur La Performance et La Prévention Des Blessures En Cyclisme. Université de Poitiers, Poitiers
11. Ericson M, Nisell R (1987) Patellofemoral joint forces during ergometric cycling. Phys Ther 67:1365–1369
12. Ericson MO, Nisell R (1986) Tibiofemoral joint forces during ergometer cycling. Am J Sports Med. https://doi.org/10.1177/036354658601400407
13. Clancy CE, Gatti AA, Ong CF, Maly MR, Delp SL (2023) Muscle-driven simulations and experimental data of cycling. Sci Rep. https://doi.org/10.1038/s41598-023-47945-5
14. Drouet J-M, Champoux Y, Dorel S (2009) Development of multiplatform instrumented force pedals for track cycling. Eng Sport 7(1):263–271. https://doi.org/10.1007/978-2-287-99054-0_32
15. Martín-Sosa E, Chaves V, Alvarado I, Mayo J, Ojeda J (2021) Design and validation of a device attached to a conventional bicycle to measure the three-dimensional forces applied to a pedal. Sensors. https://doi.org/10.3390/s21134590
16. Bouillod A, Soto-Romero G, Grappe F, Bertucci W, Brunet E, Cassirame J (2022) Caveats and recommendations to assess the validity and reliability of cycling power meters: a systematic scoping review. Sensors. https://doi.org/10.3390/s22010386
17. Dieltiens S, D'Hondt J, Juwet M, Versteyhe M (2019) Development of a low-cost measurement system to determine

3-dimensional pedal loads during in-situ cycling. Transp Probl 14:151–159. https://doi.org/10.20858/tp.2019.14.4.13
18. Balbinot A, Milani C, da Nascimento JSB (2014) A new crank arm-based load cell for the 3D analysis of the force applied by a cyclist. Sensors 14:22921–22939. https://doi.org/10.3390/s141222921
19. Boyd T, Hull ML, Wootten D (1996) An improved accuracy six-load component pedal dynamometer for cycling. J Biomech. https://doi.org/10.1016/0021-9290(95)00177-8
20. Álvarez G, Vinyolas J (1996) A new bicycle pedal design for on-road measurements of cycling forces. J Appl Biomech 12:130–142. https://doi.org/10.1123/jab.12.1.130
21. Falda-buscaiot T (2017) Analyse Biomécanique En Ski: Conception et Validation'un Nouveau Capteur d'efforts à l'interface Skieur- Environnement., Université de Grenoble Alpes
22. Pottinger MV (2018) Inverse dynamic analysis of ACL reconstructed knee joint biomechanics during gait and cycling using OpenSim
23. Koska D, Oriwol D, Maiwald C (2023) Comparison of statistical models for characterizing continuous differences between two biomechanical measurement systems. J Biomech. https://doi.org/10.1016/j.jbiomech.2023.111506
24. Koo TK, Li MY (2016) A guideline of selecting and reporting intraclass correlation coefficients for reliability research. J Chiropr Med 15:155–163. https://doi.org/10.1016/j.jcm.2016.02.012
25. Stone C, Hull ML (1995) The effect of rider weight on rider-induced loads during common cycling situations. J Biomech 28:365–375. https://doi.org/10.1016/0021-9290(94)00102-A
26. Ruby P, Hull ML (1993) Response of intersegmental knee loads to foot/pedal platform degrees of freedom in cycling. J Biomech 26:1327–1340
27. Broker JP, Gregor RJ (1990) A dual piezoelectric element force pedal for kinetic analysis of cycling. Int J Sport Biomech 6:394–403
28. Weir JP (2005) Quantifying test-retest reliability using the intraclass correlation coefficient and the SEM. J Strength Cond Res 19:231–240. https://doi.org/10.1519/15184.1
29. Burnie L, Barratt P, Davids K, Worsfold P, Wheat J (2023) Biomechanical measures of short-term maximal cycling on an ergometer: a test-retest study. Sports Biomech 22:997–1015. https://doi.org/10.1080/14763141.2020.1773916

Publisher's Note Springer Nature remains neutral with regard to jurisdictional claims in published maps and institutional affiliations.